Efficient and accurate prediction of cosite isolation on large platforms

The current trend of dense Integration of numerous electromagnetic devices onto electrically large platforms presents a significant challenge for designers. (Electrically large means that major dimensions are much larger than λ (wavelength)).

A key requirement for multi-antenna systems on a platform is maximizing cosite isolation by identifying optimal placement on a platform. Traditional empirical methods, which rely on trial-and-error testing by measuring coupling at each candidate position, are both cost-prohibitive and time-consuming. Utilizing numerical modelling techniques to predict coupling values significantly reduces the number of required physical measurements, thereby accelerating the deployment process and reducing the cost.

The mutual coupling between antennas is usually quantified by mutual *s*-parameters between antenna ports. Generally, accurate evaluation of *s*-parameters is possible by using full wave simulation methods. However, although full wave simulation methods are well developed and applicable on high power computers, there are still two major challenges in obtaining meaningful and usable results for *s*-parameters:

1) Electrically large platforms, and
2) Low-coupled antennas.

The goals of this paper are to demonstrate:

1) The effectiveness of the WIPL-D 3D EM solver in the evaluation of mutual coupling of multiple antennas mounted on electrically large platforms.
2) Tips and tricks for obtaining accurate results for far no line of sight (no LoS) antennas
3) How to create a parametric model of an airliner, which can be easily adjusted to various real-life types.

The examples used for demonstration shown in Fig. 1 are:

a) Two quarter-wavelength monopole antennas mounted on opposite faces of a metallic cube of side $0 < 2A \leq 20\lambda$, as shown in Fig. 1a, and

b) Five quarter-wavelength monopole antennas mounted on opposite sides of an airliner fuselage at a frequency of 1.06 GHz (~140 λ), as shown in Fig.1b.

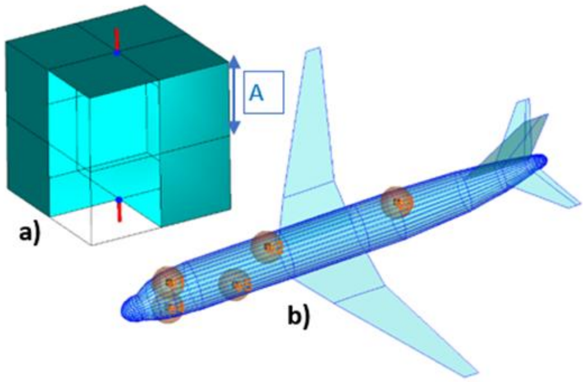

Figure 1. Monopole antennas mounted on: a) metallic cube, b) airliner.

WIPL-D 3D EM Solver: Application to Electrically Large Platforms

WIPL-D 3D EM solver is based on Method of Moments applied to Surface Integral Equation (MoM/SIE). It means that unknown quantities are electric currents spread over boundary metallic surfaces. (If there are boundary dielectric/magnetic surfaces, the unknown quantities are also equivalent electric and magnetic currents spread over these surfaces.)

The boundary surfaces are modelled by patches in the form of bilinear surfaces, i.e., quadrilaterals uniquely defined by four arbitrarily spaced nodes. Surface currents over patches are approximated by higher order basis functions of polynomial type up to order $n = 7$. In this way, maximum patch size up to 2λ can be applied, reducing the number of unknowns per λ^2 for metallic surfaces down to ~25. (Note that by using RWG basis functions over triangles of maximum size of 0.1 λ, the patch of size of 1 λ needs to be meshed into 200 triangles, requiring 300 unknowns per λ^2.) In this way, the number of unknowns, when compared with RWG bases, can be reduced up to 12 times.

The total number of unknowns required for simulation depends directly on the surface area of the platform expressed in wavelengths squared. For example, the fuselage of a typical airliner can be roughly approximated by a cylinder of length $L = 40$ m and radius $a = 4$ m. The surface area of the cylinder is $S = 2a\pi(a+L) \approx 528$ m^2. At frequency $f_0 = 1$ GHz, the wavelength is $\lambda = 0.3$ m, so that its surface area in wavelength squared is $S/\lambda^2 \approx 5865$. The number of cylinder unknowns, $N_c \approx 5865 \times 25 = 146{,}625$, represents about 70% of the number of airliner unknowns, $N \approx 200{,}000$. Finally, by using one symmetry plane, we can roughly estimate that the airliner can be simulated by using $N_0 \approx 100{,}000$ unknowns.

The number of airliner unknowns at arbitrary frequency can be estimated by a simple formula

$$N = (f/f_0)^2 N_0 \qquad (1)$$

where f_0 = 1 GHz and $N_0 \approx$ 100,000.

Generally, for a large number of unknowns, the dominant part of simulation time is due to the solution of the matrix equation. If the solution is performed by the direct LU decomposition method, the solution time can be estimated as

$$T = A N^3 / 3 \qquad (2)$$

where A is the time needed for evaluation of one summation and one multiplication. This time can be reduced if the solution is performed on GPUs (Graphics Processing Units) instead of CPUs. In this work, a single GPU card (Nvidia GeForce RTX 3080) installed on a standard desktop computer is used for the solution of the matrix equation. Table 1 shows the solution time for the matrix equation for the number of unknowns ranging from N_0 to $3N_0$.

Table 1. Matrix equation solution time on the GPU.

Number of Unknowns	*Solution time [seconds]*	*Solution time [minutes]*
100,000	184	3.07
120,000	289	4.82
140,000	409	6.82
160,000	567	9.45
180,000	784	13.07
200,000	1048	17.47
220,000	1349	22.48
240,000	1729	28.82
260,000	2103	35.05
280,000	2611	43.52
300,000	3230	53.83

Using data from the table, it is estimated that $A = 3.6 \cdot 10^{-13}$ seconds. According to formula (2), a matrix equation of $N = 1$ million unknowns can be solved in 33 hours. This time can be further reduced by using up to 8 cards in parallel installed at dual processor server. By increasing the number of unknowns, the efficiency of parallelization tends to 100%. The maximum number of unknowns tested in this way is N = 3 million, and the corresponding simulation time is 5 days. According to formula (1), it corresponds to a frequency f = 5.5 GHz, in which case the length of the airliner in wavelengths is ~770 λ.

Generally, the problems based on a large number of unknowns can be solved by using far fewer resources by applying approximate methods, e.g., Multi-Level Fast Multipole Method (MLFMM) or Domain Decomposition Solution (DDS). However, these methods are not able to give a stable solution for very low-level mutual coupling between antennas, and will not be considered in this paper.

Tips and Tricks: High accuracy of mutual s-parameters

Obtaining accurate results for very low-level mutual coupling between antennas generally requires increased computational resources. In what follows, three techniques will be elaborated:

1) Appropriate increase in the reference frequency with respect to the operating frequency
2) Adding an absorber to the interior of the platform
3) Separating antennas mutually and from the platform by air-filled bubble domains

Increase in the Reference Frequency

Meshing of the CAD model into bilinear surfaces, as well as automatic choice of expansion orders for currents spread over each bilinear surface, are performed according to the reference frequency, f_{ref}. By default, the reference frequency is equal to the operating frequency of the problem. By increasing the reference frequency above the operating frequency, the number of unknowns increases more or less according to formula (1), where $f = f_{ref}$, f_0 is the operating frequency, and N_0 is the number of unknowns at $f_{ref} = f_0$. One good way to examine the convergence of results for s-parameters (with increasing the number of unknowns) is to increase f_{ref} in predefined steps, e.g., by 30% of f_0.

The first task is to understand how to choose f_{ref} to obtain accurate results for low-level coupling between antennas mounted on a platform. For that reason, a model of two monopole antennas mounted on a metallic cube, as shown in Fig. 1a, is analysed for three values of half side length, A = 0.83 λ, A = 4.49 λ, and A = 9.50 λ. For each value of A, the simulation is performed by increasing f_{ref} according to the formula

$$f_{ref} = f_0\,(1+k \cdot MPS/A), \quad k = 0,\ldots,10 \qquad (3)$$

where Maximum Patch Size is set to MPS = 0.833 λ, MPS = 1.5 λ, and MPS = 1.5 λ, respectively to three values of A. Table 2 shows f_{ref}/f_0 for $k = 0,\ldots,10$. In this way, the number of unknowns is smoothly increased by increasing k, as shown in Fig. 2. (The number of unknowns corresponds to the quarter part of the model since two symmetry planes are used to reduce the number of unknowns.)

Table 2. Ratio of reference frequency and operating frequency for three sizes of the cube.

k	*A* = 0.83 λ	*A* = 4.49 λ	*A* = 9.5 λ
0	1	1	1
1	2.004	1.334	1.158
2	3.007	1.668	1.316
3	4.011	2.002	1.474
4	5.014	2.336	1.632
5	6.018	2.670	1.789
6	7.021	3.004	1.947
7	8.025	3.339	2.105
8	9.029	3.673	2.263
9	10.033	4.007	2.421
10	11.036	4.341	2.579

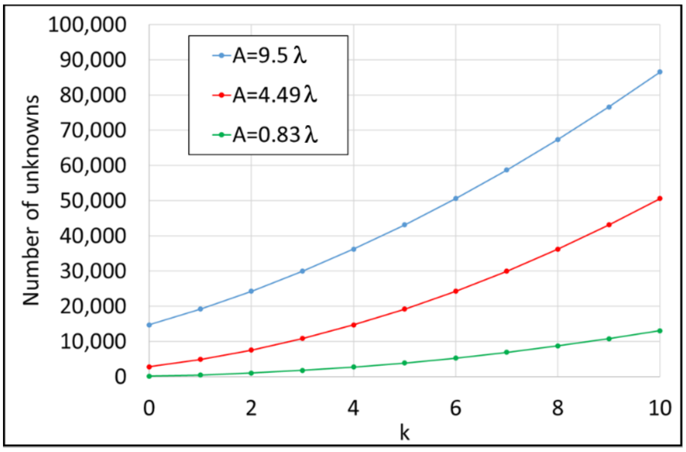

Figure 2. Number of unknowns versus parameter k, for model in Fig. 1a, for three cube sizes.

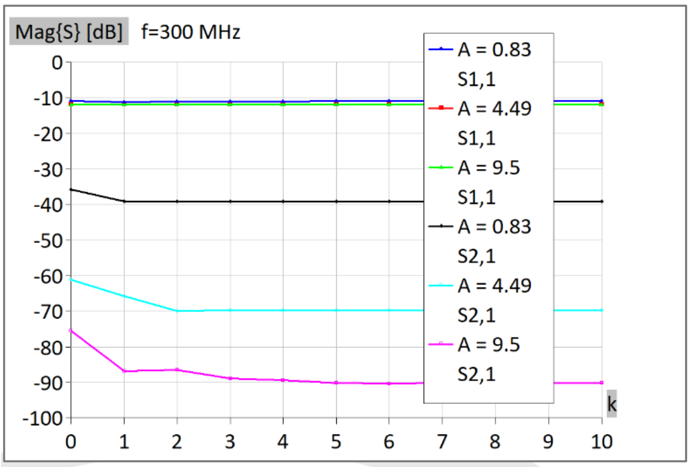

Figure 3. S_{11} and S_{21} versus parameter k, for model in Fig. 1a, for three cube sizes.

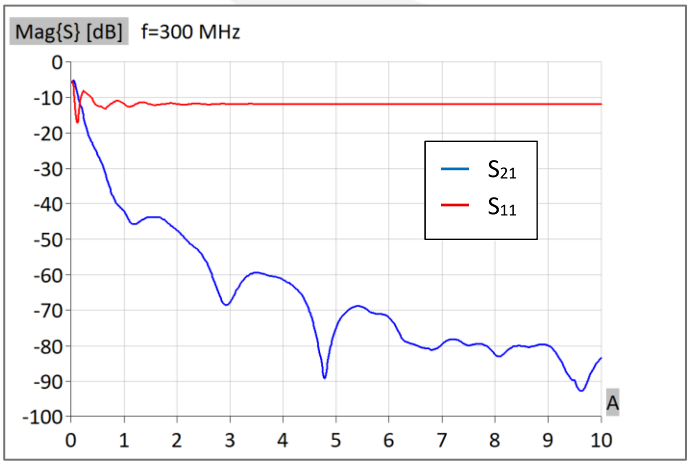

Figure 4. S_{11} and S_{21} versus A (half cube side length), for the model in Fig. 1a.

Fig. 3 shows s_{11} and s_{21}-parameters versus parameter *k*. It is seen that s_{21} for three values of *A* converged for k=1, 2, and 5, respectively. Based on these results, and many other results not published here, it is concluded that for low-level mutual coupling between antennas, results converge if the reference frequency, f_{ref}, is increased by 30% to 60% with respect to the operating frequency, f_0.

Fig. 4 shows s_{11} and s_{21}-parameters versus A (half cube side length). Fully convergent results are obtained at a reference frequency 66.7% higher than the operating frequency.

Platform with absorber

The reasons that low-level mutual coupling between antennas requires an increase in the reference frequency can be explained in the following way. Whichever SIE is used for the solution of induced currents over the platform, the boundary conditions for tangential components of electric and magnetic field over the platform surface are not fully satisfied, so that each numerical model of the platform behaves as a cavity supporting spurious EM fields. Generally, usage of HOBFs suppresses the influence of inner spurious EM fields on outer EM fields very effectively. In particular, for low-level coupling it is necessary to furthermore strengthen this suppression, which is performed by an increase in reference frequency.

An alternative way to suppress spurious EM fields inside the platform is to fill the platform with light absorbing material, e.g., with a domain whose relative electric and magnetic constants are $\varepsilon_r = \mu_r = 1 - j0.1$. For example, in the case of the model in Fig. 1, an absorber is added in the form of a cube, whose half side length is equal to B = C A, where C < 1, as shown in Fig. 5.

Generally, such a domain requires twice as many unknowns as are needed for the platform. However, the effect of absorbing the spurious EM field can be achieved even if the reference frequency of the absorber is reduced with respect to the operating frequency, e.g., from $f_{ref}/f_0 = 0.5$ to $f_{ref}/f_0 = 0.7$, so that the total number of unknowns with respect to the operating frequency is increased from 50% to 100%.

Fig. 6 shows s_{11} and s_{21} versus f_{ref}/f_0 for A=9.5 λ, for a cube with and without an absorber. It is seen from the graph that results obtained with the absorber inserted are very stable and almost constant with increasing the reference frequency. In particular, the result obtained for a reference frequency equal to the operating frequency is practically satisfactory regarding the accuracy.

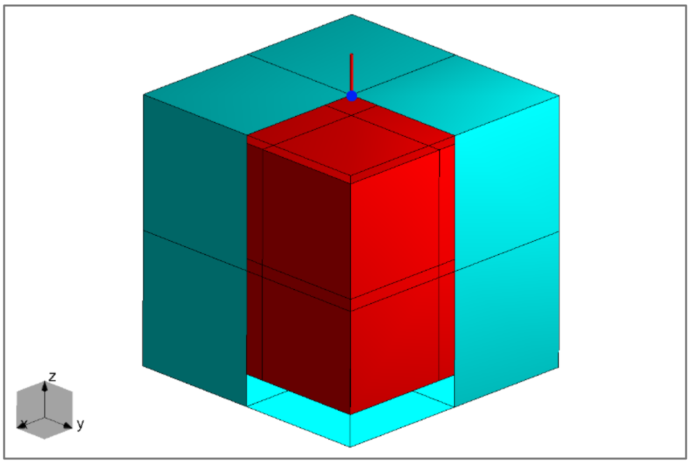

Figure 5. Metallic cube with absorber.

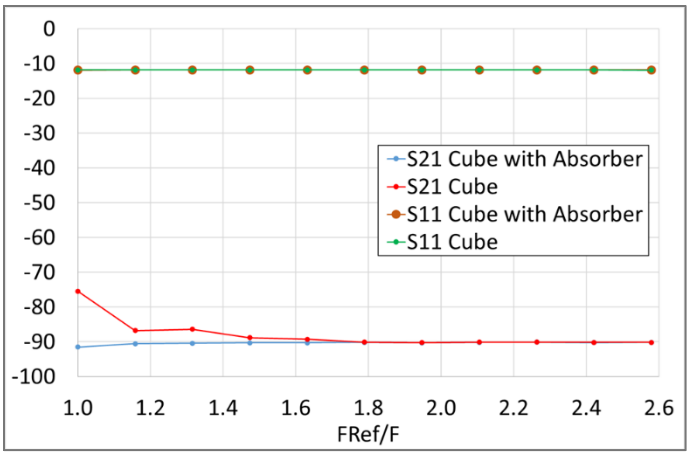

Figure 6. S_{11} and S_{21} versus f_{ref}/f_0 for A=9.5 λ, for cube with and without absorber.

Antennas encapsulated by bubbles

Alternatively, spurious EM fields inside the platform can be suppressed in the following way:

a) Each antenna is encapsulated by an artificial boundary surface in the form of a sphere (bubble), as shown in Fig. 7.
b) The new domain assigned to the interior domain of the bubble is set to be air.
c) Part of the bubble surface inside the platform is set to be made of the same metal as the platform.
d) Part of the bubble surface outside of the platform is set to be a dielectric surface between two air-filled domains.

In this way, the antennas are neither mutually coupled nor coupled by the platform through the EM fields, but by equivalent currents at the bubble boundary surfaces.

Fig. 8 shows s_{11} and s_{21} versus f_{ref}/f_0 for A=9.5 λ, for a cube with and without bubbles. It is seen from the graph that results obtained with bubbles are very stable and almost constant with increasing the reference frequency. In particular, the result at a reference frequency about 15% higher than the operating frequency are practically satisfactory in terms of accuracy.

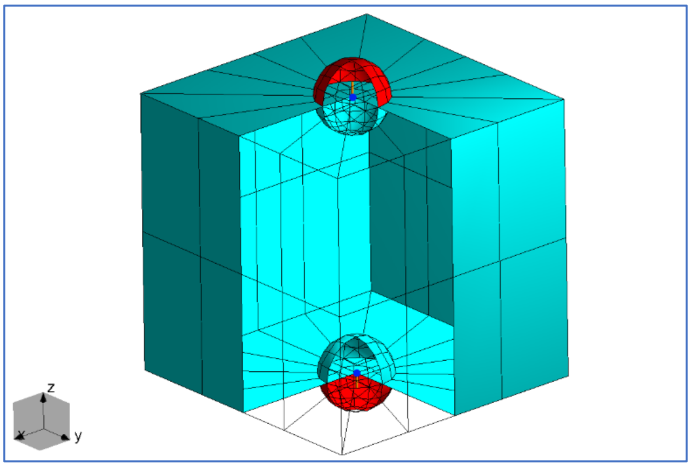

Figure 7. Antennas encapsulated by bubbles.

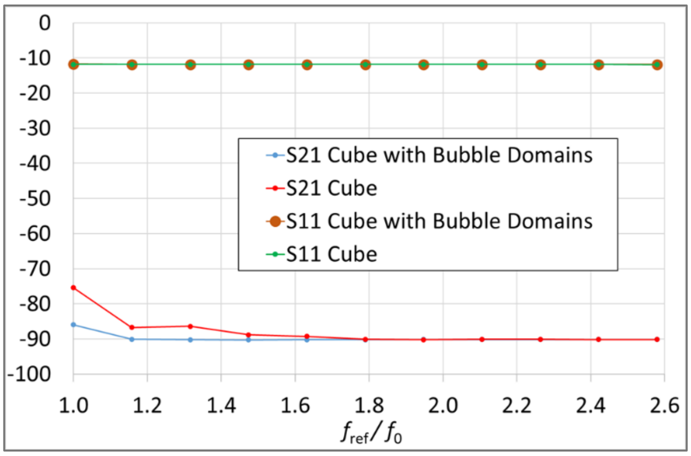

Figure 8. S_{11} and S_{21} versus f_{ref}/f_0 for A=9.5 λ, for cube with and without bubble domains.

Real-life example: Monopole antennas mounted along an airliner

Shape and dimensions of the airliner are precisely described in the addendum. Three models of airliner with five monopole antennas, basic, with absorber, and with bubble, are shown in Fig. 9. Locations and dimensions of these antennas are given in Tables 3 and 4.

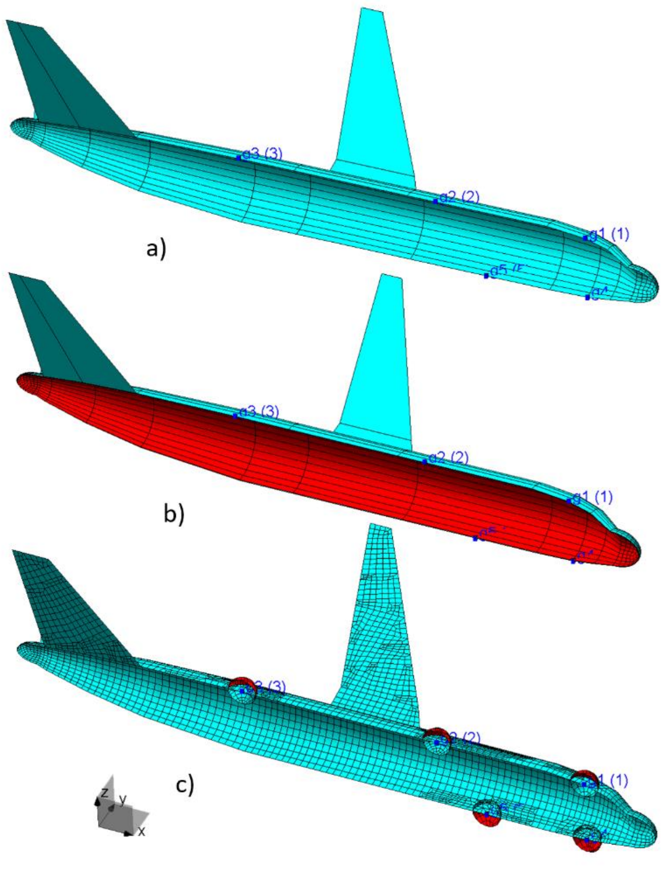

Figure 9. Model of monopole antennas placed along the airliner: a) basic, b) with absorber, and c) with bubbles.

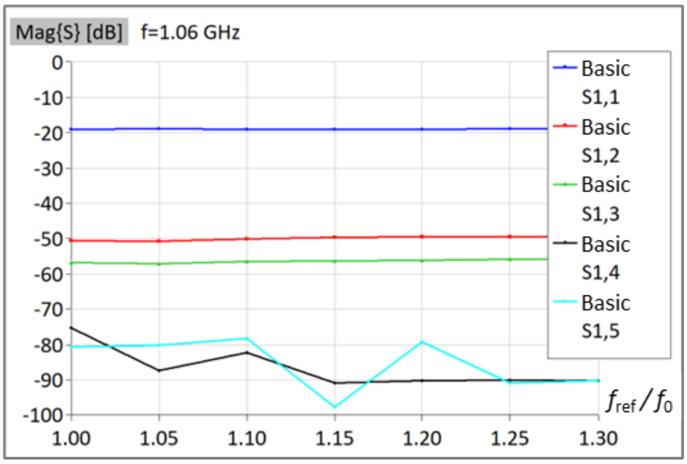

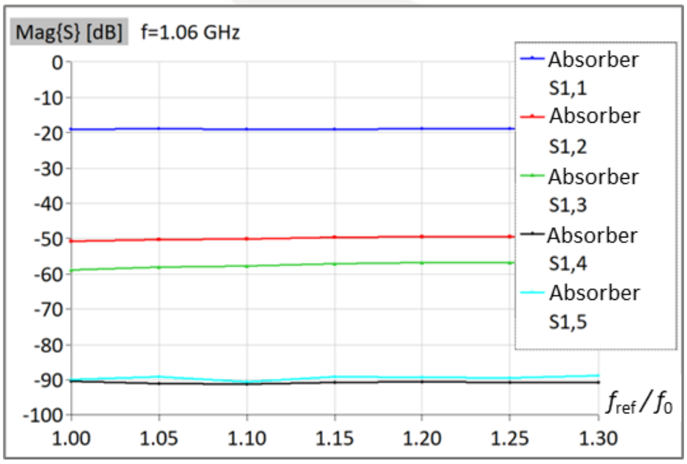

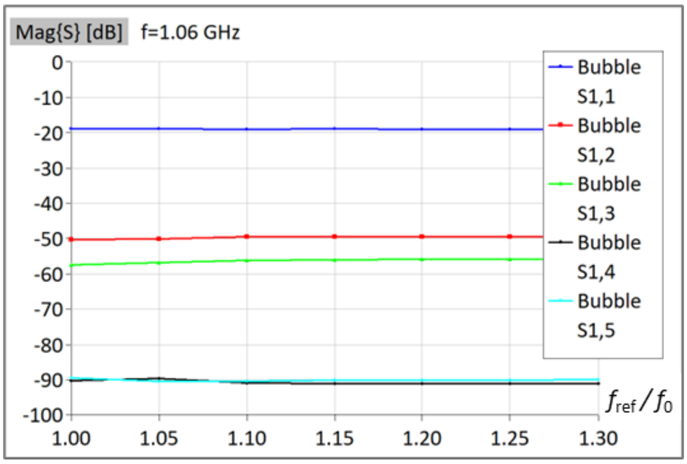

Figure 10. *S*-parameters versus ratio of reference frequency and operating frequency for three models: a) basic, b) with absorber, and c) with bubbles.

Fig. 10 shows *s*-parameters versus f_{ref}/f_0 for monopole antennas placed along the airliner fuselage. Results are presented for three models: a) basic, b) with absorber, and c) with bubbles. It is seen from the graph that results obtained with an absorber or bubbles are very stable and almost constant with increasing the reference frequency. These advanced models do not require an increase in reference frequency above the operating frequency, while the basic model requires an increase of at least 25%-30%.

Table 3. Locations of antennas.

Antenna	*X [m]*	*Z [m]*
1	17.16	1.89
2	8.118	2.25
3	-3.18	2.15
4	17.16	-2.09
5	11	-2.15

Table 4. Length and radius of the wire monopoles.

Parameter	Value [m]
Length	0.95*λ/4
Wire radius	Length/1000

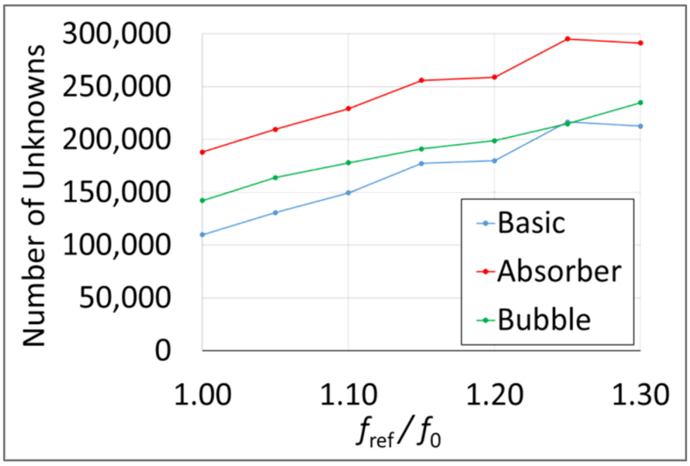

Figure 11. Number of unknowns for three airliner models: a) basic, b) with absorber, and c) with bubbles.

Fig. 11 shows the number of unknowns versus f_{ref}/f_0 for three airliner models. Having in mind the results shown in Fig. 10, it is concluded that the number of unknowns required for obtaining accurate results for all s-parameters is: a) 210,000 for the basic model, b) 190,000 unknowns for the model with absorber, and c) 145,000 unknowns for the model with bubbles. More precisely, these numbers of unknowns are necessary for no LoS antennas, s_{14} and s_{15}-parameters, while for s_{11} and LoS antennas, s_{12} and s_{13}, it is not necessary to increase the reference frequency above the operating frequency for any of the models.

Fig. 12 shows *s*-parameters versus operating frequency f_0, for five reference frequency values f_{ref}. Results are obtained by using basic models. It is seen from the graphs that for no LoS antenna, the reference frequency needs to be increased by 30% to 60% to obtain very accurate results, while for s_{11} and LoS antennas, it is not necessary to increase the reference frequency above the operating frequency.

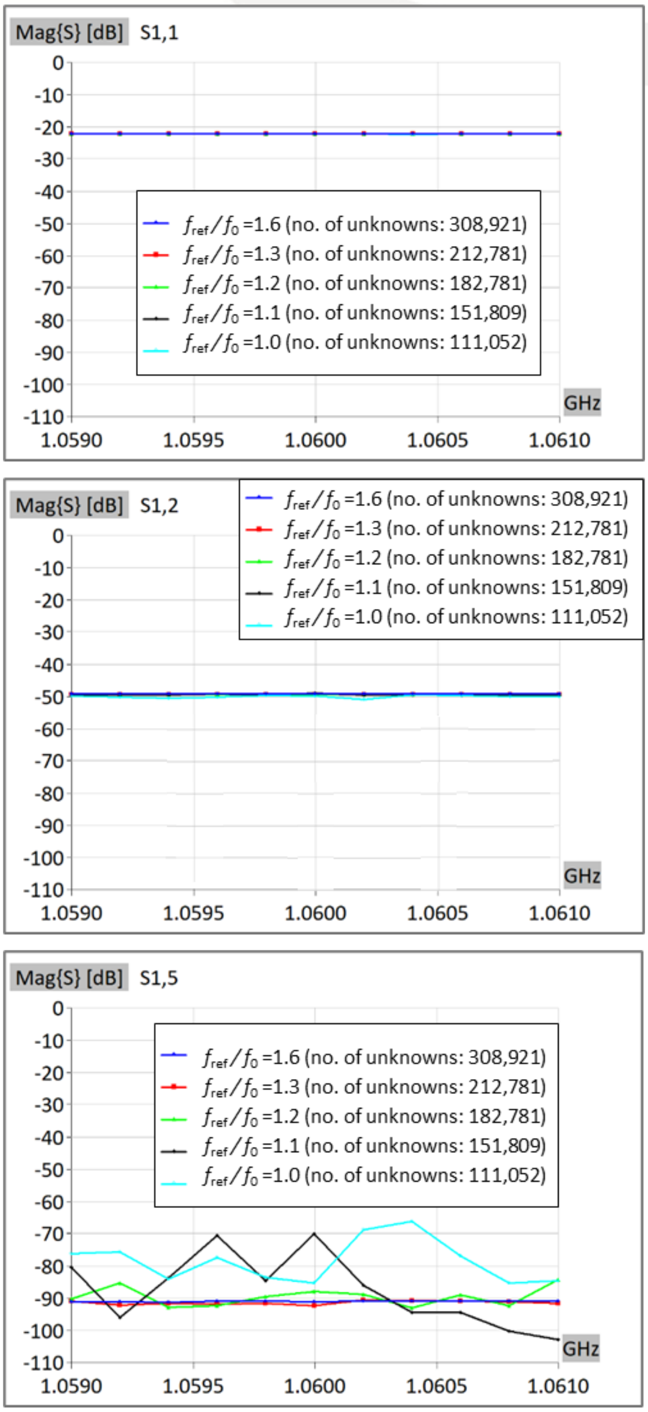

Figure 12. *S*-parameters versus operating frequency f_0, for five reference frequency values f_{ref}.

Conclusion

A study of coupling between the quarter-wavelength monopole antennas resting on the canonical shape of a cube and a realistic airliner was conducted. All simulations were performed in the WIPL-D 3D EM solver. The paper outlined detailed dimensions of the cube and the aircraft, so the results can be verified by the readers of this document, either in WIPL-D or any other software.

Particular attention is given to the simulation of electrically large platforms and low-level antenna coupling. It is shown that simulation of a basic model of antennas mounted along a 40 m long airliner operating at a frequency of 1 GHz requires 100,000 unknowns and a few minutes on a desktop computer with a GPU card. However, in order to obtain accurate results for low level antenna coupling (e.g., at levels down to -100 dB), it is necessary to increase the reference frequency by 30% to 60% above the operating frequency. In this way, the number of unknowns is increased up to 2-3 times.

To obtain accurate results for low level antenna coupling without increasing the reference frequency, two novel techniques are proposed: 1) the platform is filled with absorbing material, or 2) antennas are mutually separated and separated from the fuselage by artificial spherical boundaries (bubbles). Both techniques provide a reduction in the number of unknowns by 15% to 35%, when compared with the basic model that utilized increased reference frequency.

Addendum: Real-life model of airliner

Floor plan of airliner, tail and nose half-ellipsoids, segment of fuselage, horizontal stabilizer, vertical stabilizer, and tail are shown in Figs. A1 to A6, respectively. Airliner dimensions, dimensions of fuselage segments, and dimensions of tail and nose half-ellipsoids are given in Tables A1 to A3.

Table A1. Airliner dimensions.

Symbol	Value	Explanation
W_{Span}	35.18 [m]	*Wing Span*
W_{Base}	11.32 [m]	*Wing Base*
W_{Chord}	1.27 [m]	*Wing (Tip) Chord*
$W_{Dihederal}$	7.63 [m]	*Wing Dihedral*
W_{Sweep}	30.84 [deg]	*Wing Sweep*
W_{Alpha}	-37.5 [deg]	*Radial Angle of Wing Attachment Point*
H_{Span}	11.4 [m]	*Horizontal (Stabilizer) Span*
H_{Chord}	1.15 [m]	*Horizontal (Stabilizer Tip) Chord*
H_{Sweep}	41.1 [deg]	*Horizontal (Stabilizer) Sweep*
$H_{Dihederal}$	7.1 [deg]	*Horizontal (Stabilizer) Dihedral*
H_{Alpha}	25 [deg]	*Radial Angle of Horizontal Stabilizer Attachment Point*
T_{Height}	8.17 [m]	*Tail (Tip) Height with Respect to Fuselage Axis*
T_{Sweep}	41.57 [deg]	*Tail Sweep*
T_{Chord}	2.22 [m]	*Tail (Tip) Chord*

Table A2. Dimensions of fuselage segments.

N	*x* Position of #N Circle [m]	*z* Height of #N Circle Center [m]	*a* Radius of #N Circle [m]
0	-16.49	0.95	0.68
1	-15.90	0.84	0.84
2	-13.42	0.56	1.35
3	-10	0.26	1.81
4	-3.81	0	2.15
5	-0.45	0	2.15
6	6.43	0	2.15
7	14.87	0	2.15
8	17.16	-0.10	1.99
9	18.53	-0.24	1.69
10	19.70	-0.60	1.15

Table A3. Dimensions of nose and tail half-ellipsoids.

Symbol	Value	Explanation
c_0	1.15	*Semi-Axis of Tail Semi-Ellipsoid*
c_{10}	1.75	*Semi-Axis of Nose Semi-Ellipsoid*

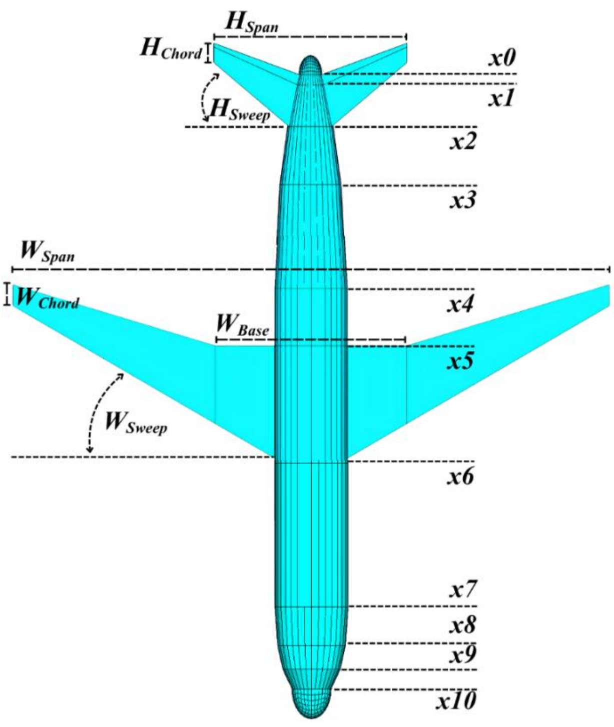

Figure A1. Floor plan of airliner.

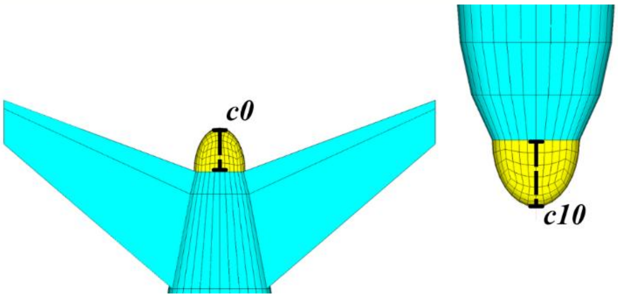

Figure A2. Tail and nose half-ellipsoids (Floor plan).

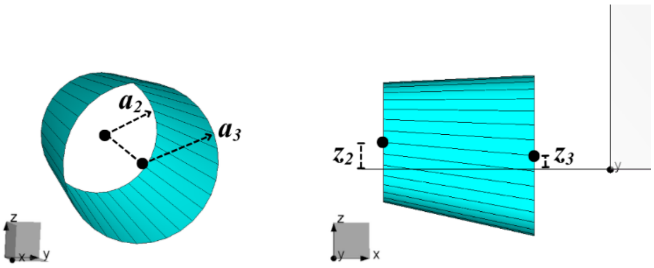

Figure A3. Typical segment of fuselage (oblique truncated cone).

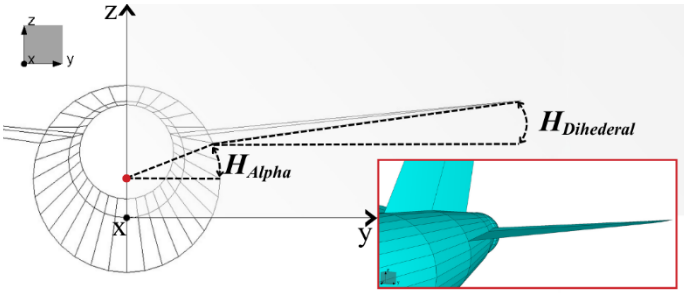

Figure A4. Horizontal stabilizer (Front view)

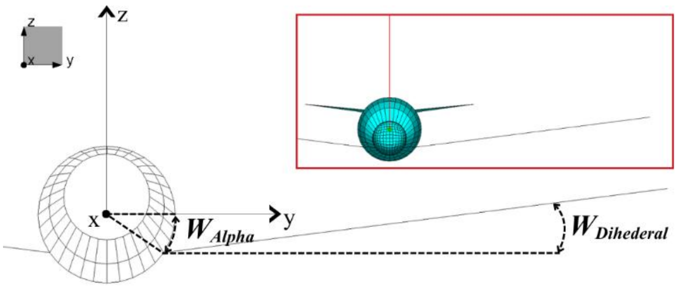

Figure A5. Wing (Front view).

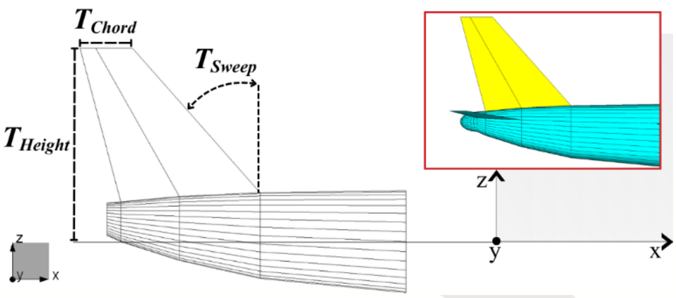

Figure A6. Tail (Side view).